Dmitriy Mikhaylov (Autor)

Ultrashort Pulse Laser Ablation of Bulk Materials Using Shaped Laser Beams

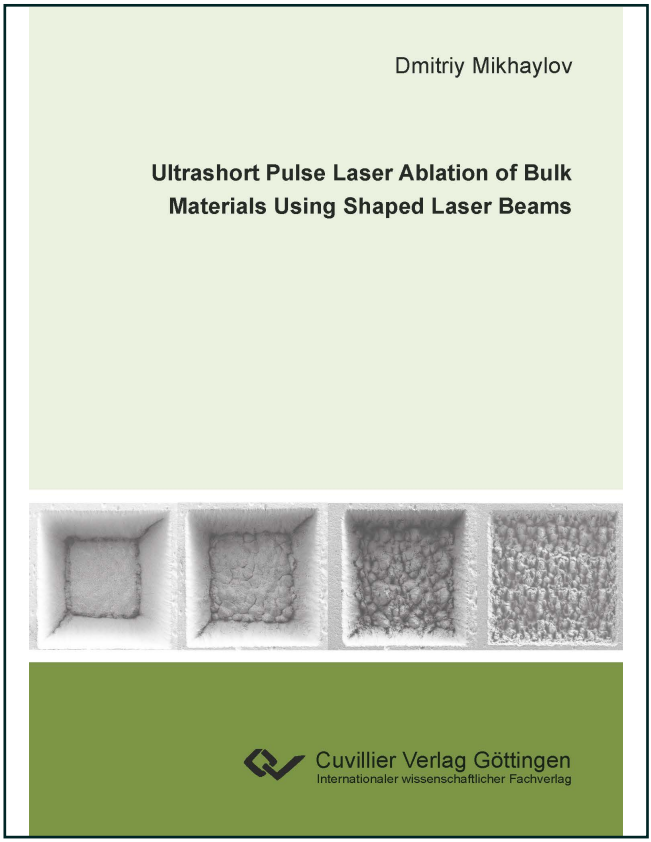

https://cuvillier.de/de/shop/publications/8466

1 Introduction

Light as a tool has been adapted by humans for thousands of years to address a wide range of applications. Light has been used as a source of heat, for communication, for measuring time, for viewing distant places or very small objects [1]. The range of applications of light grew evolutionarily with the development of mankind until a scientific breakthrough happened in the last century. Light, the wild source of energy propagating in all directions, was tamed between two resonator mirrors. The LASER principle, Light Amplification by Stimulated Emission of Radiation, was developed and implemented [2]. Mankind has now become able to generate, direct and specifically use bundled, high-energy light radiation – the laser beams.

Since the invention of laser, the development of ever new laser sources has been driving the development of ever new laser applications and vice versa. Laser beams with different wavelengths, higher power levels, shorter pulses, and better beam quality have been becoming available for utilization in new processes [3,4]. Nowadays laser can be called a truly universal, all-purpose tool. However, even though new laser sources enable new applications, the already developed laser processes are seldom optimized to their limits regarding throughput and quality.

In industrial manufacturing technology, laser sources are used for a wide range of applications, such as welding, cutting, drilling or milling [5]. The most common approach for optimization of some process is to adjust main laser parameters – power, feed rate, polarization state as well as pulse energy and repetition rate, for pulsed lasers. Changing laser wavelength or pulse duration is less simple and often linked to more complex system technology – wavelength converter or variable pulse compressor. Thus, these parameters are varied more seldom. Usage of different beam shapes for process optimizations is almost not applied in industrial environment until now. On the one hand, the generation of an arbitrary intensity distribution is not a trivial task and cannot be realized using standard system technology. On the other hand, understanding of the influence of the beam shape on a laser process often simply does not exist.

The focus of this thesis lies on the optimization of one particular process – ultrashort pulse (USP) laser ablation of metals. The USP technology is particularly favored for fabrication of functional microstructures in bulk materials, e.g. microdrilling of fuel injection nozzles, generation of hydraulic microchannels or trimming of sensors [6]. The favoritism of the USP milling process bases on its two main advantages – high ablation precision and low heat influence on the remaining bulk material. The lateral

precision is restricted only by the spot size of the focused laser beam which can be adjusted using a proper beam guiding and focusing optics. Ablation depth of each ultrashort laser pulse lies in the range of several nanometers yielding highly precise volume ablation. However, the USP technology also exhibits some limitations. One of these is the relatively low productivity represented by the volumetric ablation rate describing how much bulk volume is removed per unit of time.

An attempt to increase ablation rates of USP laser processes is presented in this thesis. To narrow the optimization task down, only ablation of small 2.5D structures from geometrically limited bodies are regarded in the current work. An example of such structures is presented in Figure 1.1 as a scanning electron microscope (SEM) image of a spray nozzle – an oil injection component for stationary heating systems. This and other similar components are manufactured by USP lasers at Bosch sites. From the production start until now, the ablation rate could not be increased even though ever new laser sources have become available. A typical value for the ablation rate of such small structures lies in the range between $0.001\,\mathrm{mm}^3/\mathrm{s}$ and $0.01\,\mathrm{mm}^3/\mathrm{s}$ and is regarded insufficient for many new applications [7].

The ablation rate of USP laser processes can only up to a certain extent be scaled up by increasing average laser power. However, the utilization of the available laser power still highly depends on each particular application and is especially limited by ablation structure and body geometries. Beam shaping, as a means of optimally distributing the available laser power on the workpiece, is seen as one of promising solutions to increase volumetric ablation rates. Thus, the current need for research is seen in the improvement of USP ablation processes by means of beam shaping.

The objectives of this thesis are to answer several research questions. It has to be investigated which strategy is capable of accelerating USP ablation processes and which potential can be raised. Furthermore, a hypothesis for a technical solution for high performance beam shaping needs to be stated. The solution should be proposed, implemented and verified. Finally, the experimental proof of the improvement of USP ablation processes by means of beam shaping has to be demonstrated.

The structure of this thesis is in line with the stated objectives. Chapter 2 provides basic information on USP laser material processes and technology. It describes main

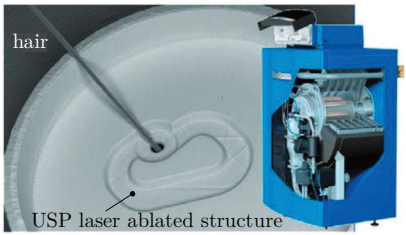

Fig. 1.1 SEM image of a spray nozzle plate (left) used in oil burners for heating systems (right). A human hair is presented for a better visualization of dimensions. The inner structure is ablated by means of USP lasers at Bosch production sites [8].

relationships between applied laser parameters and ablation rates as well as heating up of the bulk material. Furthermore, general theory on laser beam shaping is briefly discussed. After that, the core component for the flexible and programmable beam shaping used in this work, the so-called liquid crystal on silicon spatial light modulator (LCoS-SLM), is reviewed in detail. The chapter is finalized by discussing different methods and algorithms for the generation of phase holograms required for diffractive beam shaping.

Materials processed in the course of the study are named in Chapter 3 including their physical properties. Furthermore, experimental equipment used in this work, for instance laser sources as well as beam guiding and shaping elements, is reviewed. Finally, the applied qualification and characterization methods for the beam shape measurement as well as the analysis of ablation surface and volume are described.

A method for calculation of the theoretical maximum of the volumetric ablation rate for a given structure geometry from a geometrically bounded body is presented in Chapter 4. Moreover, ideal requirements on a laser source and a beam shaping optics are derived. Application of this particular system technology is discussed to maximize the volumetric ablation rate.

Especially the requirement on the ideal beam shape, which is found to be a perfectly flat top-hat of an arbitrary geometry, cannot be realized with the state of the art optics. To overcome this technical restriction, the development of a novel beam shaping concept for the generation of flat top-hat beam profiles is described in Chapter 5. Furthermore, a new method for generation of high-accuracy beam splitter profiles using LCoS-SLMs is presented. Implementation of the novel beam shaping optics as well as validation of its performance are emphasized in the last section of Chapter 5.

Experimental investigation into the question on increase of the volumetric ablation rate by using large shaped laser beams is discussed in Chapter 6. The results of the application of the novel beam shaping optics for structuring of stainless steel are presented for the scanning and stamping ablation strategies. The achievable enhancement of ablation rates and generated surface qualities are demonstrated by reference to a parameter study. A calculation scheme for the estimation of the volumetric ablation rate in dependence on the applied process parameters is given as a conclusion of the process development chapter.

This thesis is finally summarized in Chapter 7 outlining developed methods and optical concepts and depicting achieved results. An outlook for further meaningful research and development of the system and process technology is given.

2 Theoretical principles and state of the art

In order to place the reader into the right context of the ongoing research and development activities, an overview over the state of the art in ultrashort pulse laser ablation as well as laser beam propagation is given. Special attention is addressed to the LCoS-SLM based diffractive beam shaping technique, algorithms for calculation of phase holograms, and some machine learning methods, as these topics play an essential role in the presented work.

2.1 Ultrashort pulse laser technology for material processing

The technology of ultrashort pulse lasers is highly attractive for its application in the field of material processing. In industrial applications, the commonly used pulse duration range of USP lasers is from 200 fs – 50 ps. In absolute terms, these pulses carry very little energy of some microjoule and seldom of some millijoule. However, when an ultrashort laser pulse is focused on a material surface, the intensity there will lie in the range of $10^{12} - 10^{15}$ W/cm^2 for the typical beam diameters of several tens of micrometers. At these intensities and pulse duration, the entire energy is absorbed just in the uppermost surface layer. The material evaporates abruptly. Only a very locally limited volume is released from the substrate without the residual material being influenced by the laser pulse. High-precision ablation almost without any thermal influencing of the bulk is thus possible. One speaks of the so-called "cold ablation" [9].

Because a large variety of materials can be processed by USP lasers, their applications are extremely versatile. For example, eye surgeries [10], marking [11–13], drilling [6, 14, 15], cutting [16], structuring [17–19], bending [20], welding [21], or additive manufacturing of different materials [22, 23] is possible. In this thesis, application of USP lasers in industrial environments with a special focus on micro-structuring of bulk metals is considered.

2.1.1 Single pulse ablation

When a single ultrashort laser pulse hits material surface, different effects take place, as illustrated in Figure 2.1. Due to the exposure to an electric wave of high intensity, material surface overheats abruptly. Shock waves are emitted into the bulk and into

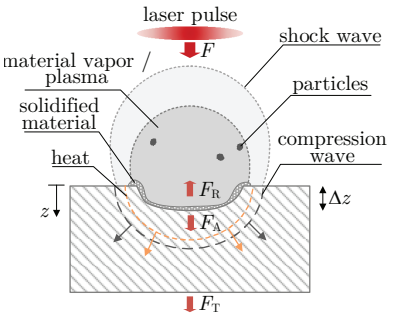

Fig. 2.1 Schematic illustration of the single pulse ablation process. The fluence F of the laser pulse is absorbed F_A by material, reflected F_R from the surface, or transmitted F_T through the body. The absorbed fluence is partly used for material ablation and partly absorbed in form of heat. The ablated material is evaporated or spalled as nano- and micro-particles and is either removed by e.g. suction or recasts in the surroundings. The material vapor is accompanied by a plasma cloud over the ablation surface. Shock waves are induced into the atmosphere and into the body by each laser pulse. A small dimple of depth Δz is created.

the atmosphere. When the induced pulse fluence exceeds the ablation threshold, some absorbed energy is used to evaporate and to chip the material. Vapor, plasma cloud and spalled particles arise over the exposed surface [24–26]. Furthermore, some part of the absorbed energy is transferred into bulk material in form of heat.

From the initial fluence F, one part is reflected (R), one part is absorbed (A), and one part can be transmitted (T): $F = F_R + F_A + F_T$. The reflected part depends on many factors, such as material itself, laser wavelength, surface inclination (Fresnel equations), surface condition (roughness), to name the most significant. The non-reflected part is absorbed by the substrate, whereas the absorbed fluence decreases with the depth z according to the Beer-Lambert law:

$$F(z) = F_0 \cdot e^{-\alpha z}, \tag{2.1}$$

with $F_0 = F - F_R$ being the absorbed fluence at the surface and α standing for the absorption coefficient.

The absorption coefficient α defines the optical penetration depth $\delta = 1/\alpha$, which is the depth where the initially absorbed pulse fluence is reduced to the value F_0/e. For metals, values of optical penetration depth lie in the range of several hundredths of the applied laser wavelength [27, 28]. Thus, the transmitted part of the fluence can be neglected, when materials with a thickness in micrometer range or larger are processed by near infrared radiation.

As discussed in [29], the ablation depth of one pulse can be derived from the Beer-Lambert law:

$$\Delta z_p = \delta \ln\left(\frac{F}{F_{th}}\right). \tag{2.2}$$

The ablation depth Δz_p corresponds to the depth at which the absorbed fluence is just equal to the threshold fluence F_{th}. Its value is defined for a not yet laser treated

surface. However, the threshold fluence can change with each laser pulse, which is known as the incubation effect. In addition, this value is also influenced by the body temperature [30,31]. Here, F is defined as the total induced fluence instead of using the absorbed term F_0. This is legitimate due to the respective definition of the threshold fluence term F_{th}.

The ablation depth has to be integrated over the cross-section of the beam profile to calculate the material volume ablated per laser pulse ΔV_{p}:

$$\Delta V_{\mathrm{p}} = \iint \Delta z_{\mathrm{p}}(x,y)\mathrm{d}x\mathrm{d}y = \delta \iint \ln\left(\frac{F(x,y)}{F_{\mathrm{th}}}\right)\mathrm{d}x\mathrm{d}y. \tag{2.3}$$

If the laser beam profile is an ideal top-hat with the cross-sectional area A_{TH}, the volume ablated per pulse ΔV_{TH} is calculated by:

$$\Delta V_{\mathrm{TH}} = A_{\mathrm{TH}} \cdot \delta \ln\left(\frac{F}{F_{\mathrm{th}}}\right) = A_{TH} \cdot \delta \ln\left(\frac{E_{\mathrm{p}}}{A_{\mathrm{TH}} \cdot F_{\mathrm{th}}}\right). \tag{2.4}$$

When a Gaussian beam is used, which in most cases much better represents the reality, the ablation depth must be integrated over the Gaussian fluence distribution resulting in the volume ablated per laser pulse ΔV_{G} [32]:

$$\Delta V_{\mathrm{G}} = \frac{\pi w_0^2}{4} \cdot \delta \ln^2\left(\frac{2F}{F_{\mathrm{th}}}\right) = \frac{\pi w_0^2}{4} \cdot \delta \ln^2\left(\frac{2E_{\mathrm{p}}}{\pi w_0^2 \cdot F_{\mathrm{th}}}\right), \tag{2.5}$$

where w_0 is the Gaussian waist radius in the focal plane and E_{p} is the total incident pulse energy. The fluence F of the Gaussian beam is defined as an average value and is equal to the pulse energy divided by the Gaussian cross-section $F = E_{\mathrm{p}}/(\pi w_0^2)$.

2.1.2 Principles to increase the volumetric ablation rate

Great research effort is being done in scientific and industrial communities to increase throughput of ultrashort pulse laser machining. Main parameters for the enhancement of laser ablation processes are pulse fluence, laser repetition rate, pulse duration, wavelength, burst mode, and finally laser beam shape [31–42].

In a simplified perception, the volumetric USP ablation rate $\dot{V}_{\mathrm{abl}}$ is a product of the volume ablated per laser pulse ΔV_{p} from Equations (2.3) to (2.5) and the pulse repetition rate f_{rep}:

$$\dot{V}_{\mathrm{abl}} = f_{\mathrm{rep}} \cdot \delta \iint \ln\left(\frac{F(x,y)}{F_{\mathrm{th}}}\right)\mathrm{d}x\mathrm{d}y, \tag{2.6}$$

For top-hat and Gaussian beams, the formulae are expressed in Equations (2.7) and (2.8), respectively:

$$\dot{V}_{\mathrm{TH}} = f_{\mathrm{rep}} \cdot A_{\mathrm{TH}} \cdot \delta \ln\left(\frac{F}{F_{\mathrm{th}}}\right) = f_{\mathrm{rep}} \cdot A_{\mathrm{TH}} \cdot \delta \ln\left(\frac{E_{\mathrm{p}}}{A_{\mathrm{TH}} \cdot F_{\mathrm{th}}}\right), \tag{2.7}$$

$$\dot{V}_{\mathrm{G}} = f_{\mathrm{rep}} \cdot \frac{\pi w_0^2}{4} \cdot \delta \ln^2\left(\frac{2F}{F_{\mathrm{th}}}\right) = f_{\mathrm{rep}} \cdot \frac{\pi w_0^2}{4} \cdot \delta \ln^2\left(\frac{2E_{\mathrm{p}}}{\pi w_0^2 \cdot F_{\mathrm{th}}}\right). \tag{2.8}$$

Based on Equations (2.7) and (2.8), free process parameters for scaling up of the ablation rate $\dot{V}_{\mathrm{abl}}$ are the fluence F or the pulse energy E_{p}, the pulse repetition rate f_{rep} as well as the beam size and shape A_{TH} or w_0. The optical penetration depth δ is not a free parameter, but can be changed e.g. by adjusting pulse duration or wavelength. Increase of the volumetric ablation rate can be done by raising all of the mentioned parameters. However, the scale-up attempt is not unlimited. The boundaries are set by process or system limitations. Heat accumulation is one of the process limiting effects and will be discussed in the next section. From the point of view of system technology, a rather low beam deflection velocity or poor beam shaping technology are the typical examples for the limiting factors.

The term of the so-called optimal fluence plays a great role in the optimization of USP laser ablation processes. To introduce it, a graph of energy efficiency ξ_{p} is plotted over the quotient between the applied fluence F and the threshold fluence F_{th} in Figure 2.2. Here, the therm of energy efficiency is defined as a relation between the material volume that is ablated per single laser pulse (cf. Equations (2.4) and (2.5)) and the applied pulse energy $\xi_{\mathrm{p}} = \Delta V_{\mathrm{p}}/E_{\mathrm{p}}$. For comparison reasons, the spot sizes are set equal, $A_{\mathrm{TH}} = \pi w_0^2$. Due to its shape, flanks of a Gaussian beam contain energy that does not contribute to the ablation being lower than process threshold. A Gaussian beam shape is hence less efficient than a top-hat profile.

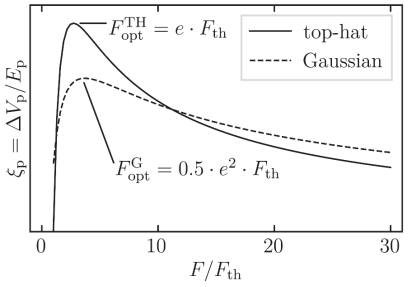

Fig. 2.2 Ablation efficiency ξ_{p} of Gaussian (solid) and ideal top-hat (dashed) beam profiles plotted over the ratio of the applied fluence and the threshold fluence F/F_{th}. The beam cross-sections are identical, $A_{\mathrm{TH}} = \pi w_0^2$.

Each curve has a global maximum, which represents the theoretical optimum fluence for the maximum ablation efficiency. Processing at this fluence should lead to the

maximum ablation rate while other parameters are kept constant. For top-hat and Gaussian beams, the fluence values are derived from Equations (2.4) and (2.5) as:

$$F_{\mathrm{opt}}^{\mathrm{TH}} = e \cdot F_{\mathrm{th}}. \tag{2.9}$$

$$F_{\mathrm{opt}}^{\mathrm{G}} = \frac{e^2}{2} \cdot F_{\mathrm{th}}. \tag{2.10}$$

Similar considerations can be done e.g. for finding the optimal repetition rate at the given laser power and beam size in the focal plane [43].

Applied ablation strategies also play their role for scaling-up of volumetric ablation rate but are not considered in the simplified Equations (2.6) to (2.8). First of all, the boundary conditions that limit the process need to be understood. Then, the optimal process strategy can be defined resulting in the requirement for a suitable system technology.

2.1.3 Heat accumulation effects and heat transfer

The share of the absorbed pulse energy which does not contribute to the material ablation remains inside the bulk in form of residual heat. In addition, laser-induced plasma also heats-up the substrate surface. Consequently, the bulk material warms up. The exact share of laser pulse energy that is absorbed in form of heat α_{heat} depends on many process parameters. Its value is difficult to estimate and should therefore be measured in experiments, e.g. by means of calorimetry [44].

As mentioned in the introduction chapter, heat accumulation inside the bulk material is recognized to be the main limiting factor for the attempts to increase the volumetric ablation rate. This is especially the case for the processing of materials with low thermal conductivity, e.g. for USP laser cutting of glass fiber reinforced plastics [45, 46]. For metals, Bauer *et al.* stated that if some material specific critical surface temperature T_{crit} is reached during the USP laser structuring process, the ablation quality decreases [47]. Formation of the so-called bumps is observed and no flat or smooth surface is achievable. In addition, a higher concentration of oxygen was found at surfaces when T_{crit} was exceeded during the USP processing. When higher repetition rates were applied, the authors had to increase the scanning velocity accordingly, in order to prevent degradation of the surface.

The share of the laser power, which is absorbed by the bulk material as heat is:

$$P_{\mathrm{heat}} = \alpha_{\mathrm{heat}} \cdot E_{\mathrm{p}} \cdot f_{\mathrm{rep}}, \tag{2.11}$$

with α_{heat} being the heat absorption coefficient.

The surface is not further heated between the individual laser pulses. Rather, it is cooled by different mechanisms – convection, heat conduction and radiation. Since normally no medium flows around the processed surface, convection can be neglected. Heat conduction transports the induced heat from the surface to the cooler inner or surrounding material. The driving force is the temperature gradient in the body according to:

$$q_{\mathrm{cond}} = -h \cdot \nabla T, \tag{2.12}$$

where q_{cond} determines the heat flux inside body, h is the thermal conductivity and ∇T is the temperature gradient. Radiation transfers the body heat to the environment as per the Stefan-Boltzmann law:

$$q_{\mathrm{rad}} = \sigma_{\mathrm{B}} \cdot \epsilon \cdot \left(\Theta^4 - \Theta_{\mathrm{amb}}^4\right), \tag{2.13}$$

with q_{rad} being the radiation heat flux. $\sigma_{\mathrm{B}} \approx 5.7 \times 10^{-8}\,\frac{\mathrm{W}}{\mathrm{m^2K^4}}$ is the Boltzmann constant and ϵ is the emissivity of the body. Θ and Θ_{amb} determine the absolute body temperature and the absolute ambient temperature, respectively.

A simple comparison shows that for the examined case of the USP laser ablation of metals, radiation can be neglected. Metal surface can be heated up to e.g. $\Theta = 1000\,\mathrm{K}$, which reflects the reality for USP laser ablation with moderate fluences. The thermal conductivity of stainless steel is approximately $h \approx 20\,\frac{\mathrm{W}}{\mathrm{m \cdot K}}$ [48]. If the ambient and the initial body temperatures are $\Theta_{\mathrm{amb}} = \Theta_0 = 300\,\mathrm{K}$, the body thickness is 1 mm, and the maximum possible surface emissivity is $\epsilon = 1$, heat conduction is 250 times higher than radiation. Hence, the total laser induced heat from Equation (2.11) can be assumed to be conducted inside the body without being radiated or convected:

$$Q_{\mathrm{cond}} = -h \cdot \oint_S \nabla T \mathrm{d}S = -P_{\mathrm{heat}}, \tag{2.14}$$

where Q_{cond} denotes the conduction heat and S is the conduction surface.

As mentioned before, some critical temperature is the main limiting material property for scaling-up of USP laser ablation processes. In order to estimate the temperature distribution in the body, it is meaningful to simulate heat accumulation processes inside the bulk material. By means of simulation, optimal laser process parameters can be determined more easily.

2.1.4 Ablation strategies

In the field of fuel injection or in automotive industry in general, USP lasers are often used for manufacturing of microstructures with lateral dimensions in the range of several hundreds micrometers to several millimeters and several tens or hundreds microns in depth, as will be discussed in Chapter 4. The ablated volume of such structures